IOSR Journal Of Applied Physics (IOSR-JAP)
e-ISSN: 2278-4861.Volume 14, Issue 4 Ser. I (Jul. – Aug. 2022), PP 52-59
www.Iosrjournals.Org

Effect of Metal Oxides Ratio on the Properties of SnO_2/Al_2O_3 Nanocomposites

S. A. Hussein [1], S. M. Gehad [2], A. A. Ebnalwaled[2*]
[1] *Physics Department, Faculty of Science, South Valley University, Qena, 83523 Egypt*
[2]*Electronics & Nano Devices Lab, Physics Department, Faculty of Science, South Valley University, Qena, 83523 Egypt.*

Abstract
Tin oxide SnO_2, Aluminum oxide Al_2O_3nanoparticles and SnO_2/Al_2O_3 nanocomposites were successfully synthesized hydrothermally at 150°C for 24hrs. The crystalline phase, morphology and particle sizes had been characterized by X-ray diffraction (XRD) and HRTEM.It is found that the particle size of the SnO_2/Al_2O_3 nanocompositesis below 30 nm,while for 50%SnO_2 & 50% Al_2O_3 it is over 30 nm. The optical properties of the prepared samples are investigated, the results showed that the energy band gap was increased by increasing Al_2O_3 ratio. The electrical properties showed that theac conductivity and the dielectric constant of the prepared samples were decreased with increasing the frequency.

Key words: *SnO_2, Al_2O_3 , nanocomposites*

Date of Submission: 12-08-2022 Date of Acceptance: 27-08-2022

I. Introduction

Semiconductor metal oxides in the form of nanocrystal behave differently from their corresponding bulk state such as ZnO, Al_2O_3, SnO_2, TiO_2 and In_2O_3. The properties of these materials have been studied due to their importance in many applications such as sensors,optoelectronic devices, solar cells and thin film transistors[1- 2].

Nano Metal oxides andits composites are well-known for their structural and high optical transmittance in the UV-Vis region and high IR reflectance[3-6].

Improvement of the structural and optical properties depends on the composition, size and surface area of the nanomaterials. Therefore, the composite of a hard nanostructured materials, such as SnO_2 and Al_2O_3 looks promising to produce an excellent composite. Nanocomposites have been synthesized via various methods, such as sol-gel processing, laser ablation, and hydrothermal route.

Among these techniqueshydrothermal method,which is one of the most commonly used methods for preparation of nanomaterials. In this method, the formation of nanomaterials can be controlled from morphology, size and properties of the prepared materials. In this method, a wide temperature range from room temperature to very high temperatures

So the aim of this work is to synthesize SnO_2,Al_2O_3,and SnO_2/Al_2O_3 nanocomposites by facile, effective, and surfactant-free hydrothermal method. Studying the morphology, microstructure, dielectric constant and optical properties will be investigated.

II. Experimental

2.1 Materials

SnO_2,Al_2O_3 and SnO_2/Al_2O_3nanocomposites were prepared usingtin oxide SnO_2(99%,ALDRICH),sodium hydroxide NaOH (AppliChem Panreac), Aluminum isopropoxide $C_6H_{21}ALO_3$(LOBA HEMIE), and distilled water.

2.2 Sampels preparation

2.2.1 Preparation of SnO_2 nanoparticles

Homogeneous solution of sodium hydroxide were prepared in an aqueous media by dissolved it in distilled water and stirred for 15 min.

Tin oxide (SnO_2) material was kept under constant stirring at room temperature using magnetic stirrer at 1100 rpm and sodium hydroxide solution was added to the SnO_2 drop by drop. The reaction was still on the stirrer for 1 hr.after complete addition of sodium hydroxide. We put the resulting gel in the autoclave at 150ºC for 24 hours. The white precipitation was washed with distilled water for several times (after 24 hours). Then the precipitations were dried in oven at 75 °C to obtain white powder.

2.2.2 Synthesis of Al_2O_3 nanoparticles

For AL_2O_3 nanoparticles preparation, Aluminum isopropoxide [$C_6H_{21}ALO_3$] (0.5 moles, 5.1062gm.) was dissolved in deionized water (160 ml). The solution was kept under constant stirring at room temperature using a magnetic stirrer at 1100 rpm for 4 hrs. to be precipitated. Then we put the resulting gel in the autoclave at 150ºC for 24 hours. The white precipitation was washed with distilled water for several times (after 24 hours).The precipitations were dried in the oven at 75°C to obtain white powder.

2.2.3 Synthesis of SnO_2/ Al_2O_3 nanocomposite

SnO_2/Al_2O_3nanocomposites were prepared using hydrothermaltechnique. By adding Al_2O_3 solution to$SnO_2$by 25%, 50%, 75% respectively drop by drop using magnetic stirrer at 1100 rpm and then was kept on it for 1 hr. The resulting mixture putted in the autoclave at 150ºC for 24 hours. The powder was washed by distilled water, and then dried at 75°C for 10 hours.

2. Characterization

The phase purity and the structure ofSnO_2, $Al_2O_3$and SnO_2/Al_2O_3 nanocomposites were characterized by X-ray powder diffraction (XRD) using (Bruker, D8 DISOVER).Further structural analysis for studying morphology and particle size of the prepared samples were investigated using (JEOL, JEM-2100 – Japan) high resolution transmission electron microscopy (HRTEM).The absorption spectra of SnO_2, Al_2O_3 and SnO_2/Al_2O_3 nanocompositeswere studied at normal incidence at room temperature in thewavelengthrange 200–900 nm with double beam UV spectrophotometer (Specord 200 Plus, Germany).The HIOKI 3532-50 LCR meter was used for studying the electrical properties ofSnO_2, Al_2O_3, and SnO_2/Al_2O_3nanocomposites measurement over the frequency range from 42 Hz to 5 MHz and temperature (298-473°k).

III. Results & Discussion

3.1 X-Ray diffraction

(XRD) patterns of SnO_2,Al_2O_3 and SnO_2/Al_2O_3 nanocomposites were studied as shown in Fig. 1Miller indices (hkl) of the diffraction peaks of SnO_2, Al_2O_3 and SnO_2/Al_2O_3 nanocompositeshave been matched with JCPDS Cards No. 002-1340 and 056-1186.

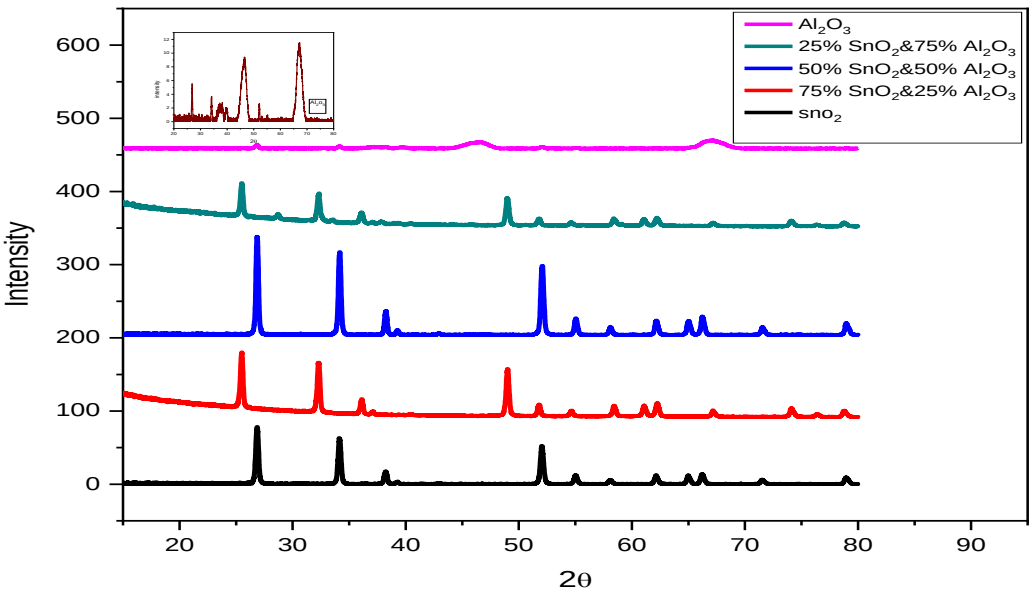

Fig. 1XRD spectra of SnO_2, Al_2O_3, SnO_2/Al_2O_3 nanocomposites.

XRD patterns show that the nanoparticles are in the tetragonal phase. The crystal size is calculated by a Scherer formula [7,8].

$$\mathbf{D = \frac{k\,\lambda}{\beta \cos \theta}}$$

Where D is the average crystallite size, λ is the applied X-ray wavelength, and k=0.94 which is a constant, θ is the diffraction angle in degree and β is the full width at half maximum (FWHM) of the diffraction peak

observed in radians. As seen from table (1),It is found that the particle size of the SnO_2, Al_2O_3 and SnO_2/Al_2O_3 nanocompositesis below 30 nm while for 50%SnO_2 & 50% Al_2O_3 it is over 30 nm, indicating that alumina can effectively prevent SnO_2 from further growing up.

Williamson–Hall analysis is the simplest method to separate the contributions of crystallite size and microstrain

$$\beta = \beta_D + \beta_\varepsilon$$

Where β is considered as the sum of the peak width due to the microstrain and the crystallite size.

For the separation, the different dependence is utilized: the size broadening is proportional to $\cos^{-1}\theta$and the strain broadening is proportional to tanθ, as shown in Fig. 2 so Williamson–Hall equation can be given as[9]:

$$\beta\text{Cos }\theta=\frac{0.94\,\lambda}{D}+4\varepsilon\,\sin\theta$$

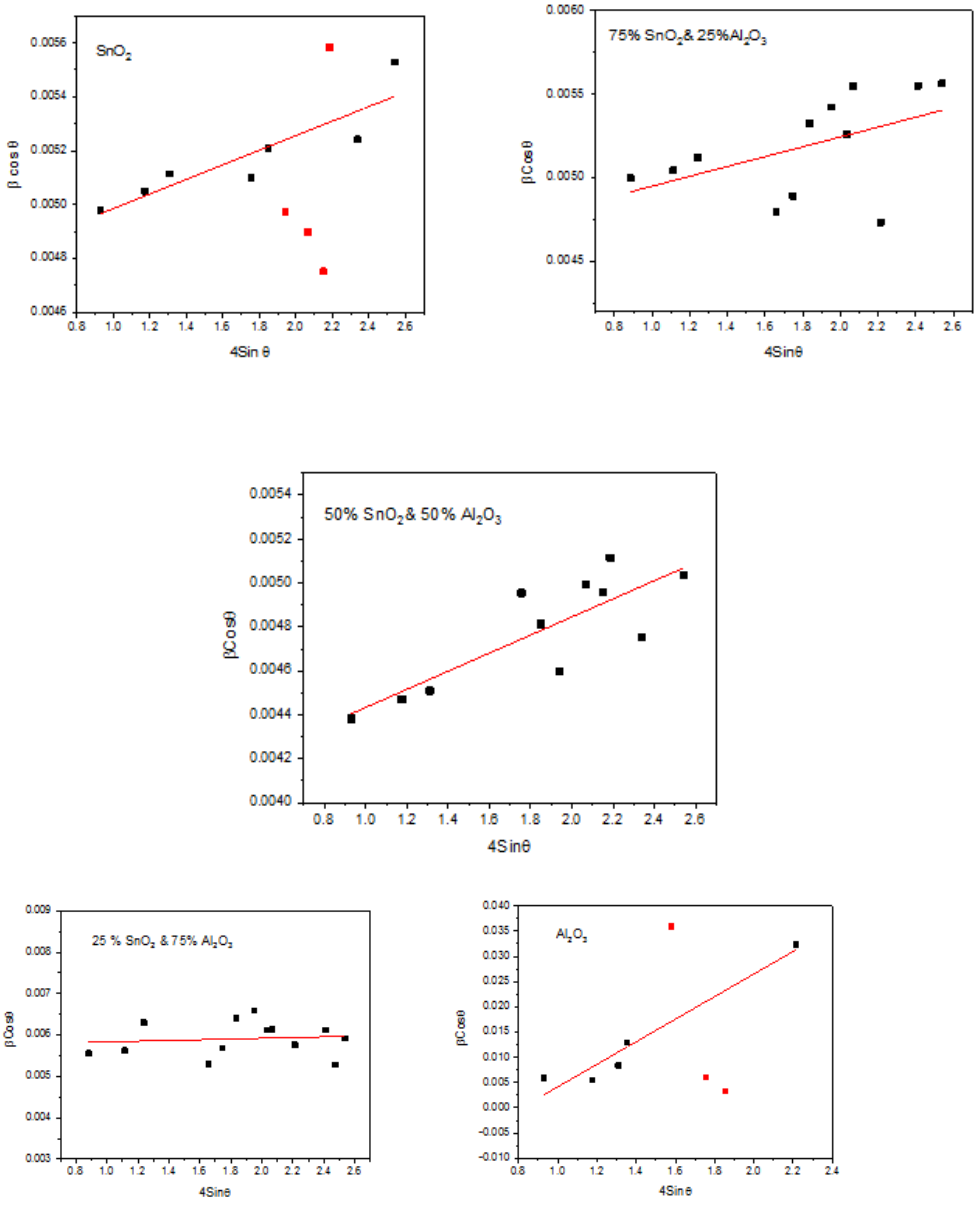

Fig. 2Williamson-Hall plot for SnO_2, Al_2O_3, SnO_2/Al_2O_3 nanocomposites.

Observation from XRD is shown in table 1 showsa comparison between the lattice parameters for the obtained nanoparticles and the lattice parameters for the standard tetragonal crystals. The comparison showed a good agreement with the standard crystals.

Sample	**SnO_2**	**75%SnO_2 &**	**50%SnO_2 &**	**25%SnO_2 &**	**AL_2O_3**

			25%AL_2O_3	**50%AL_2O_3**	**75%AL_2O_3**	
Crystallite size (nm) by Scherrer		28.29362	28.1879	30.374	23.189	21.46
Crystallitesize (nm) by waliamson		29.438	29.818	34.491	24.113	**16.085**
Strain*(10^{-4})		2.7	2.94	4.11	0.8	**147.5**
a (A˚)	**SnO_2**	4.7107	4.744236	4.29487	4.36863	
	Al_2O_3		7.400206	7.658283	7.990193	7.546094
c (A˚)	**SnO_2**	3.17492	3.17492	3.17106	3.17492	
	Al_2O_3		19.88736	21.01176	21.02488	21.02872
c/a (A˚)	**SnO_2**	0.6729	0.6692	0.73834	0.72675	
	Al_2O_3		2.6874	2.7435	2.6313	2.7867

Table (1)Comparison between SnO_2/Al_2O_3 nanocompositesparameters.

3.2 HRTEM Analysis

Fig.3 a,b,c,d and e shows the HRTEM images of SnO_2, Al_2O_3 and SnO_2/Al_2O_3 nanocomposites which is the best direct way to investigate nanoparticle size and shape. From HRTEM analysis, the primary particle size of the powder has been found to be approximately in the range of (20-80) nm. From these images, distribution of particle size of the powder is not uniform. It may be due to agglomeration of particles during the preparation of the samples.

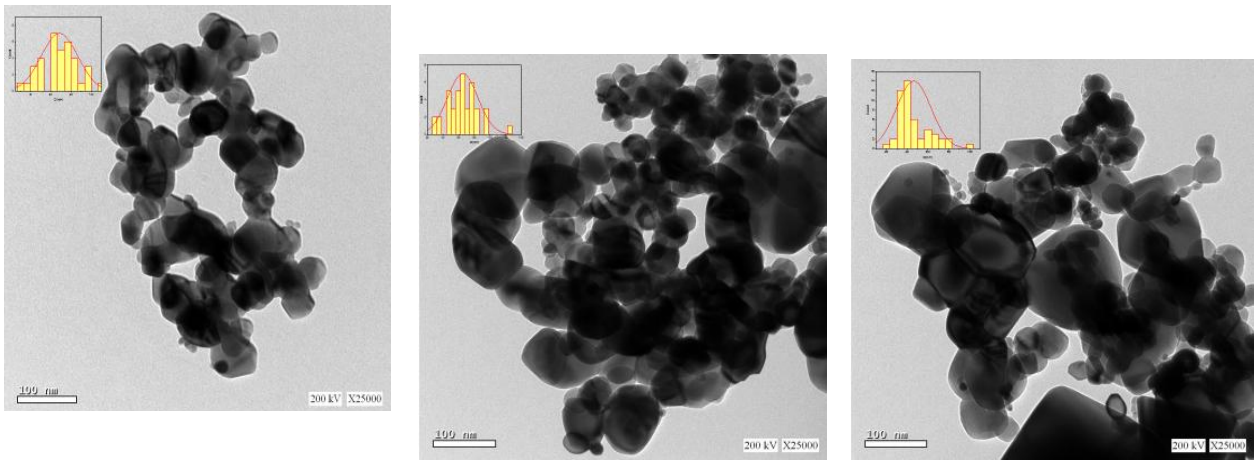

(a) (b) (c)

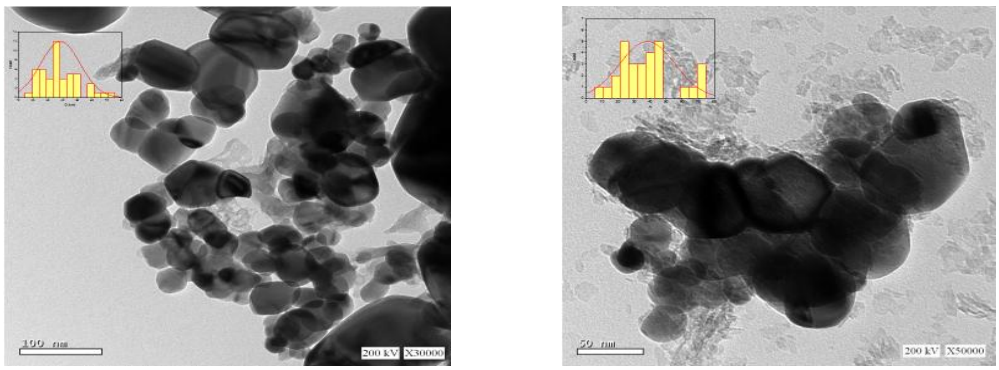

(d) (e)

Fig.3HRTEM photographs(a),(b),(c),(d) and (e)of adding Al_2O_3on SnO_2 nanoparticles by 0 %,25%, 50%, 75% and 100% respectively.

3.3 Optical properties

Absorbance measurements at near normal incidence were performed over a spectral ranging between 200 and 900 nm, Fig. 4 (a). The shapes of the curves were similar although differences in absorption were observed. With increasing the wavelength the absorption is decreased and

The absorption onset of the grown SnO_2, Al_2O_3 and SnO_2/Al_2O_3 nanocompositessamples can be assigned to the direct transition of electrons in the samples which confirms the semiconducting nature of the samples[10].

The direct optical band gap with direct transition can be calculated using the relation.[11]

$$\alpha h\upsilon = B(h\upsilon - Eg)^{1/2}$$

Where hυ is the photon energy and B is a constant that depends on the transition probability, a is the absorption coefficient and Eg is the optical band gap.

The direct band gap (E_g) of our sample was measured from the absorption coefficient data as a function of wavelength using Tauc relation thereby extrapolating the straight line of the $(\alpha h\nu)^2$ vs. hν plot to intercept on the horizontal photon energy axis and were found to 3.66,3.67,3.68,3.69 and 3.711 eVrespectively as shown in Fig. 4(b).

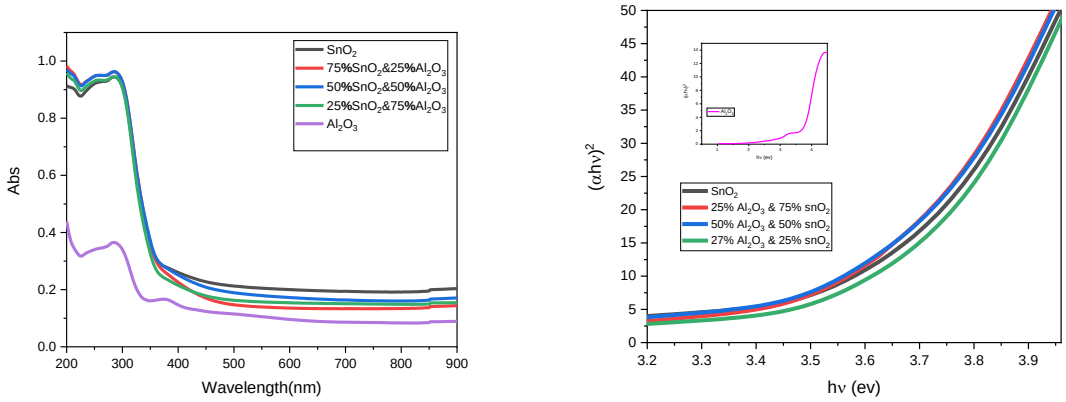

(a) (b)

Fig.4 optical properties of SnO_2, Al_2O_3 and SnO_2/Al_2O_3 nanocomposites

3.4 Electrical properties

Ac conductivity which is frequency dependent conductivity. The σ_{ac} (ω) obeys the Almond-West universal power law in the form of:

$$\sigma_{ac}(\omega) = A_0\omega^s$$

Where ω is the angular frequency ω =2 πf, s is the frequency exponent, A_0 is a constant and f is the operating frequency. The value of s can be determined from the linear slope of log σ_{ac} (ω) versus log ω and dielectric constant can be determined by $\varepsilon' = cd/A\varepsilon_0$

Where cis the capacitance of the parallel plate capacitor, $\boldsymbol{\varepsilon}_0$ is the permittivity of the free space,A is the area of parallel conducting plates and d is the separation between parallel conducting plates

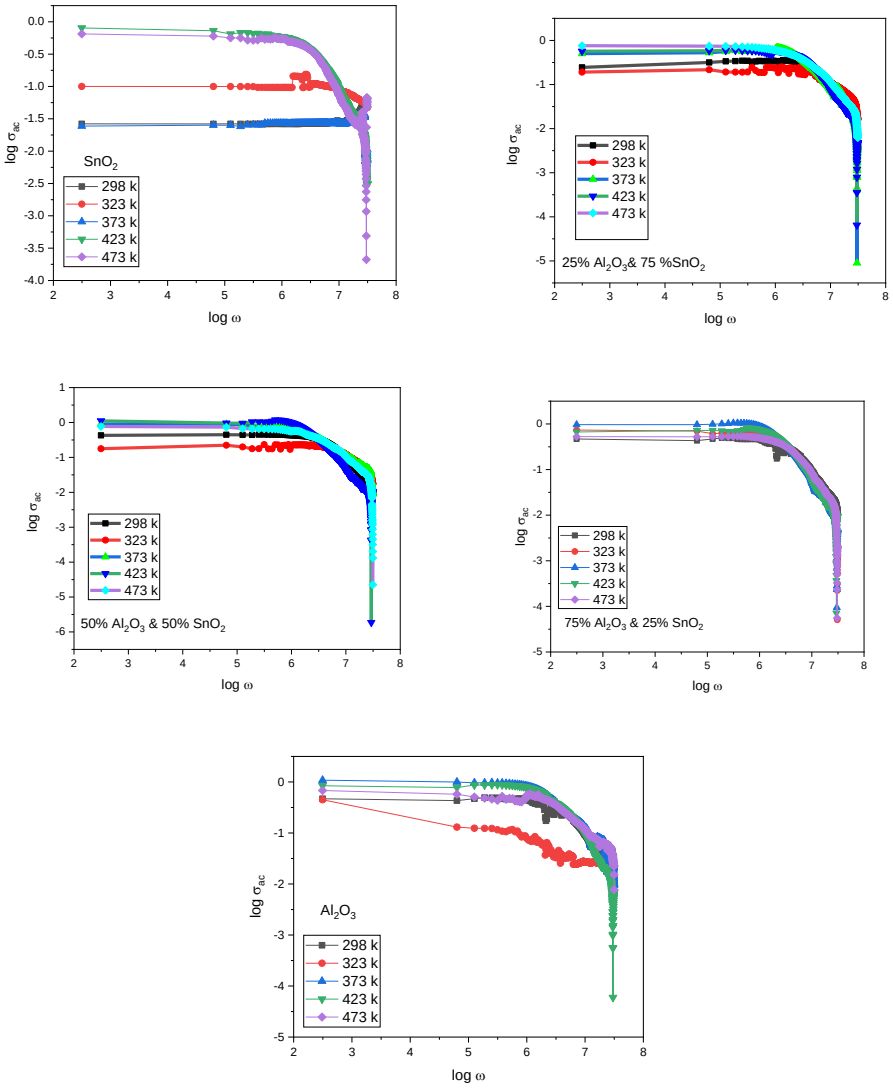

Fig.5ac conductivity at different temperature as a function of angular frequency for SnO_2/Al_2O_3 nanocomposites.

Fig.5 shows the typical ac conductivity behavior for the prepared SnO_2, Al_2O_3 and SnO_2/Al_2O_3 nanocomposites samples at different temperatures. It's observed that at low frequencies, the sample exhibits a frequency independent conductivity. This can be attributed to the random diffusion of charge carriers via hopping [12]. But at high frequencies σ_{ac} is decreased with increasing the frequency. As the temperature increased the ac conductivity increased.

The dielectric properties of SnO_2, Al_2O_3 and SnO_2/Al_2O_3 nanocompositeswere investigated in the frequency range 42-5 MHz and in temperature range 298 - 473K.

It is clear from fig. 6 that ε` decreases with increasing frequency and then achieves almost a constant value in the frequency region. The decrease of ε` with frequency can be attributed to the fact that at low frequencies ε` for polar our material is explained by the contribution of multicomponent of polarization electronic, ionic, dipolar or orientation and space charge.

A dielectric characteristic study of the grown samples indicates its response to an applied electric field. Variations in the dielectric constant ε` may be attributed to different types of polarization, which may come into play at different stages of its responses to varying temperature and frequency of the applied alternating field.Also, the obtained results indicate that the values of ε` increase with temperature at all frequencies leads to the conclusion that rise of dielectric constant for the obtained samples with temperature may be due to increase in contribution from space charge polarization with temperature[13, 14] .

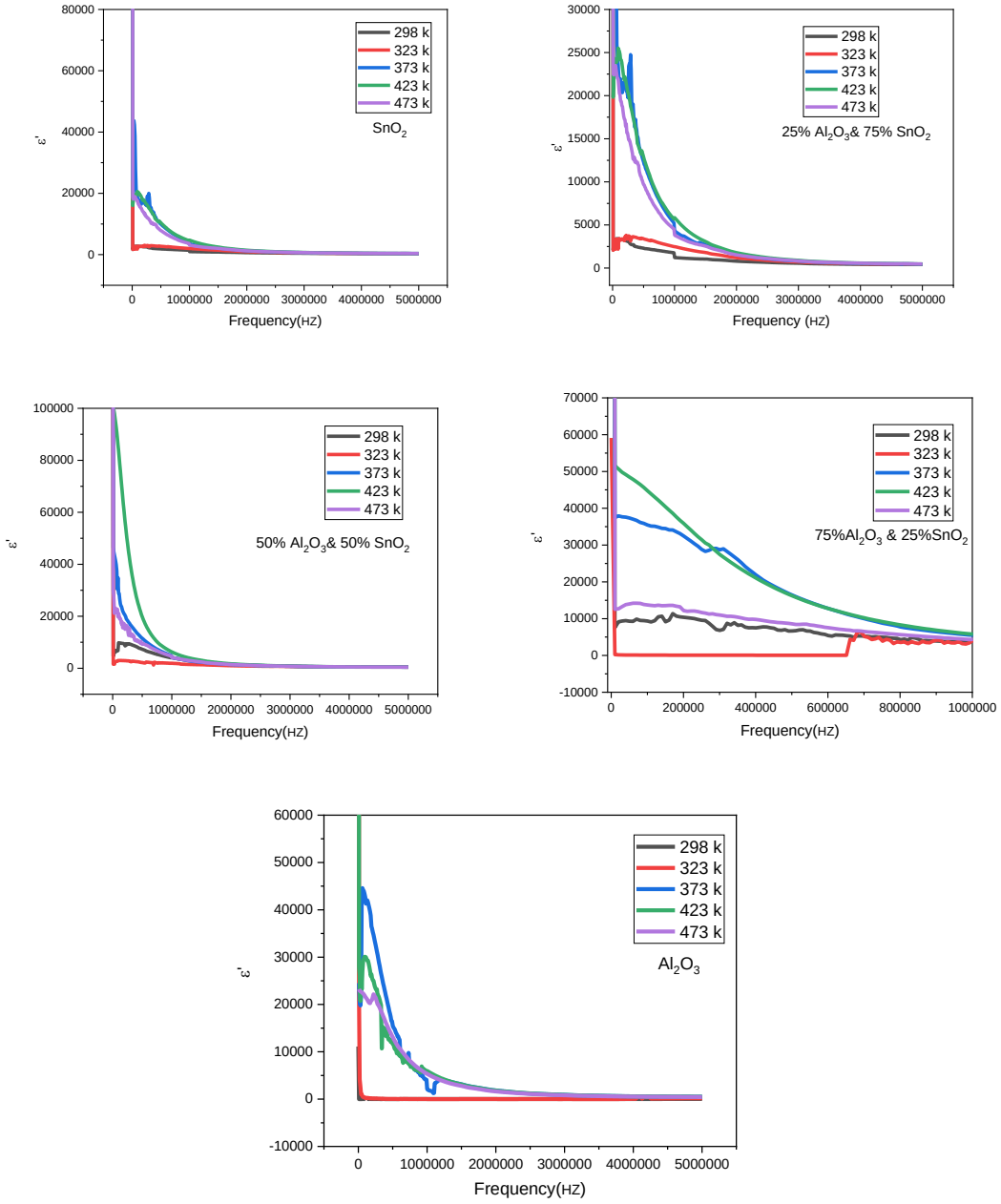

Fig.6The dielectric constant at different temperature as a function of angular frequency for SnO_2/Al_2O_3 nanocomposites.

IV. Conclusion

SnO_2/Al_2O_3 nanocomposites were synthesized using facile, effective, and surfactant-free hydrothermal method. The crystallinity, crystallite size and the morphology of the prepared samples are studied by x-ray diffraction. The yield, crystallinity, crystallite size and other observed characteristic properties indicate that the used method is suitable and economical for obtaining SnO_2/Al_2O_3 nanocomposites. The absorption and optical band gap were enhanced for the grown SnO_2/Al_2O_3 nanocomposites.For future work we plan to use the obtained samples to fabricate humidity sensors.

References

[1]. C. G. Granqvist, "Transparent conductors as solar energy materials: A panoramic review," *Sol. Energy Mater. Sol. Cells*, vol. 91, no. 17, pp. 1529–1598, 2007, doi: 10.1016/j.solmat.2007.04.031.

[2]. T. J. Coutts, D. L. Young, and X. Li, "Characterization of transparent conducting oxides," *MRS Bull.*, vol. 25, no. 8, pp. 58–65, 2000, doi: 10.1557/mrs2000.152.

[3]. T. S. Films, "A T I N OXIDE T H I N F I L M SENSOR WITH HIGH E T H A N O L," vol. 169, pp. 51–56, 1989.

[4]. M. M. Bagheri-Mohagheghi and M. Shokooh-Saremi, "The influence of Al doping on the electrical, optical and structural properties of SnO2 transparent conducting films deposited by the spray pyrolysis technique," *J. Phys. D. Appl. Phys.*, vol. 37, no. 8, pp. 1248–1253, 2004, doi: 10.1088/0022-3727/37/8/014.

[5]. N. K. Mishra, C. Kumar, A. Kumar, M. Kumar, P. Chaudhary, and R. Singh, "Structural and optical properties of SnO2-Al2O3 nanocomposite synthesized via sol-gel route," *Mater. Sci. Pol.*, vol. 33, no. 4, pp. 714–718, 2015, doi: 10.1515/msp-2015-0101.

[6]. H. Hosono, "Recent progress in transparent oxide semiconductors: Materials and device application," *Thin Solid Films*, vol. 515, no. 15 SPEC. ISS., pp. 6000–6014, 2007, doi: 10.1016/j.tsf.2006.12.125.

[7]. A. Razeghizadeh, M. Mahmoudi Ghalvandi, F. Sohilian, and V. Rafee, "The effect of substrate on structural and electrical properties of Cu3N thin film by DC reactive magnetron sputtering," *Phys. Chem. Res.*, vol. 5, no. 3, pp. 497–504, 2017, doi: 10.22036/pcr.2017.72959.1348.

[8]. E. H. de Faria, A. L. Marçal, E. J. Nassar, K. J. Ciuffi, and P. S. Calefi, "Sol-Gel TiO2 thin films sensitized with the mulberry pigment cyanidin," *Mater. Res.*, vol. 10, no. 4, pp. 413–417, 2007, doi: 10.1590/s1516-14392007000400015.

[9]. G. K. Williamson and W. H. Hall, "X-ray line broadening from filed aluminium and wolfram," *Acta Metall.*, vol. 1, no. 1, pp. 22–31, 1953, doi: 10.1016/0001-6160(53)90006-6.

[10]. N. Beloufa *et al.*, " First-Principles Calculations of the Structural, Electronic and Optical Properties of Yttrium-Doped SnO 2 ," *Ann. West Univ. Timisoara - Phys.*, vol. 63, no. 1, pp. 40–56, 2021, doi: 10.2478/awutp-2021-0004.

[11]. M. J. Deen and P. K. Basu, "Optical Processes," *Silicon Photonics*, pp. 69–108, 2012, doi: 10.1002/9781119945161.ch4.

[12]. P. Zu *et al.*, "Ultraviolet spontaneous and stimulated emissions from ZnO microcrystallite thin films at room temperature," *Solid State Commun.*, vol. 103, no. 8, pp. 459–463, 1997, doi: 10.1016/S0038-1098(97)00216-0.

[13]. S. H. Wemple and M. DiDomenico, "Behavior of the electronic dielectric constant in covalent and ionic materials," *Phys. Rev. B*, vol. 3, no. 4, pp. 1338–1351, 1971, doi: 10.1103/PhysRevB.3.1338.

[14]. M. M. El-Nahass, A. A. M. Farag, E. M. Ibrahim, and S. Abd-El-Rahman, "Structural, optical and electrical properties of thermally evaporated Ag2S thin films," *Vacuum*, vol. 72, no. 4, pp. 453–460, 2004, doi: 10.1016/j.vacuum.2003.10.005.